

Strong disorder RG for the many-body localized phase

Benjamin Villalonga Correa

May 9, 2017

Abstract

The strong disorder renormalization group offers a theoretical approach to the study of the dynamical properties of local, disordered lattice models. It has been recently applied to the problem of many-body localization, where it provides compelling results that are in agreement with the exotic properties found in these systems through numerical studies.

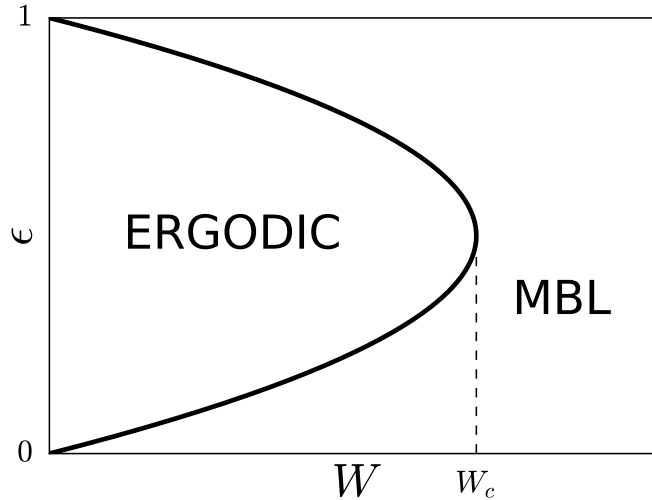


Figure 1: Typical phase diagram for the MBL transition. ϵ is the energy density of an eigenstate, which is the energy rescaled between the boundaries given by the ground state and the anti-ground state. W is the strength of the disorder in the lattice.

1 Introduction

Non-interacting, quantum, disordered systems can give rise to the phenomenon of Anderson localization. Such systems have been intensely studied in the last decades, both theoretically and computationally. Their non-interacting nature makes them tractable from a computationally point of view. In the presence of interactions, though, the study of the phenomenon of many-body localization presents much challenging difficulties. Most of the results known to the day rely on computational techniques, which for quantum interacting systems are vastly limited by the capabilities of classical computers. The systems that are computationally tractable are too small to offer a clean interpolation to the thermodynamic limit, experiments are difficult to realize, and theoretical approaches able to confirm the findings of numerical simulations are extremely valuable [5].

The one-dimensional Hamiltonians usually studied in the context of MBL present a phase diagram similar to the one on Fig. 1. Highly excited eigenstates follow a transition from an ergodic phase at low disorder strength to an MBL one at higher disorder strength. In that sense, the MBL phase can be regarded as a dynamical one, since the time evolution of a state in the system will include regions in the Hilbert space of excited eigenstates. Some dynamical

properties of these systems are among the exotic phenomenology the the MBL phase presents. The entanglement entropy between subsystems of a system originally in a state with no entanglement grows extremely slowly in time, as opposed to a linear entanglement growth that a generic system would show. At the same time, a state that is prepared in some configuration (say of spins) will decohere at slow rates, in contrast with usual non-localized systems. Also, correlations after a quench travel very slowly in the system, as opposed to the linear propagation of correlations found in generic systems quantum systems. Many more characterizations of MBL systems are found in the literature, but in this paper we will focus on the three presented.

The exotic properties that MBL systems present have called some attention in the last years. On the one hand, the slow decoherence of the states sounds appealing for quantum technologies. On the other hand, the properties found challenge the usual conceptual picture of thermalization in a system, and they offer an interesting field where a better understanding of the phenomenology is needed. Although MBL systems are far from being realizable in a real material, due to the coupling of the electrons with the phonons, there have been some attempts to simulate them in either arrays of superconducting qubits and ultra-cold atoms. The latter implementation was realized in Ref. [6]. In the same respect, the computationally intractable generalization of the problem to two dimensions was realized experimentally in Ref. [1], although this time on a bosonic lattice.

2 The model

I will restrict this paper to the model studied in Ref. [7], *i.e.* an XXZ spin-1/2 (one-dimensional) chain with no external magnetic field:

$$H = \sum_i \frac{J_i}{2} (S_i^+ S_{i+1}^- + S_i^- S_{i+1}^+ + 2\Delta_i S_i^z S_{i+1}^z), \quad (1)$$

where $S_i^z = (1/2)\sigma^z$ in the z -basis and $S^\pm = (\sigma^x \pm i\sigma^y)/4$, and the couplings J_i and the anisotropy parameters Δ_i are sampled from two uncorrelated probability distributions. The distribution of J_i has width W and the distribution of Δ_i is bounded by $(-1, 1)$. The Hamiltonian in Eq. (1) has total spin symmetry, which means equivalently that $[H, \sum_i S_i^z] = 0$, that the eigenstates of H have well defined total spin, or that H applied to a state contained in a particular total spin sector will give as a result a vector in the same sector. Note that the J_i and Δ_i parameters can be seen as a bond between two sites, and in particular J_i will be referred to as the strength of the exchange coupling of bond i .

A Jordan-Wigner transformation maps the model in Eq. (1) onto a Hamiltonian of spinless fermions. The parameters J_i represent then hopping and $J_i\Delta_i$ becomes an interaction parameter.

3 Strong disorder renormalization group

The strong disorder renormalization group, or SDRG, was first developed by Daniel Fisher along three papers [2, 3, 4] for the study of the dynamics of ground states of spin chains with disorder. More recently, the same ideas have been applied to the study of the dynamics of highly excited states on interacting, quantum spin chains with disorder [7, 8]. We will focus on the results of Ref. [7], although those in Ref. [8] follow very similar arguments.

3.1 Idea

The rationale behind the SDRG is as follows. Given a closed, quantum system described by the Hamiltonian in Eq. (1), its time evolution is given by the unitary operator:

$$e^{-iHt} = 1 + (-i)Ht + (-i)^2 H^2 t^2 + \dots, \quad (2)$$

where H is the sum of terms defined over all the bonds in the chain. If the coupling parameters J_i are drawn from a wide random distribution, then there will be a bond at $i = I$ with a much larger coupling than those in the rest of the system, and the Hamiltonian H can be separated in:

$$H = H^0 + H^1, \quad (3)$$

where:

$$\begin{aligned} H^0 &\equiv \frac{J_I}{2} (S_I^+ S_{I+1}^- + S_I^- S_{I+1}^+ + 2\Delta_I S_I^z S_{I+1}^z) \\ H^1 &\equiv \sum_{i \neq I} \frac{J_i}{2} (S_i^+ S_{i+1}^- + S_i^- S_{i+1}^+ + 2\Delta_i S_i^z S_{i+1}^z) \end{aligned} \quad (4)$$

and $\|H^0\| \gg \|H^1\|$. In such a case, the short time evolution will be dominated by H^0 , as can be seen from Eq. (2), and only the spins I and $I + 1$ around the bond I will effectively evolve, with a fast frequency characterized by the strength of J_I , which we will call Ω . This approximate time evolution is reasonable for times of the order of Ω^{-1} . For times longer than this time scale, time-dependent perturbation theory is applied, with H^1 being the perturbation around H^0 . The fast time evolution of the spins at bond I is averaged when

studying the new time scale, and we are left with the time evolution for the remaining spins given by an effective Hamiltonian of the form of the original H from Eq. (1). At this point, the spins I and $I + 1$ have been decimated. This allows us to derive the RG rules for an RG move and to iteratively access longer and longer time scales. Let's look at this in some detail.

3.2 RG moves

We start with an initial state $|\phi\rangle_0 \equiv |\uparrow\downarrow\uparrow\downarrow\dots\rangle$. The reason for choosing an antiferromagnetic state is both the fact that such state has a high expectation value for the energy in the energy spectrum (see the Hamiltonian in Eq. (1)) and that the RG moves are going to simplify greatly with such choice.

The Hamiltonian H^0 from Eq. (4) divides the Hilbert space in four eigensectors, namely $\{(|\uparrow\downarrow\rangle + |\downarrow\uparrow\rangle)/\sqrt{2}, (|\uparrow\downarrow\rangle - |\downarrow\uparrow\rangle)/\sqrt{2}, |\uparrow\uparrow\rangle, |\downarrow\downarrow\rangle\}$ at positions $I, I + 1$. However, the time evolution of the original state, which is a superposition of the states $(|\uparrow\downarrow\rangle + |\downarrow\uparrow\rangle)/\sqrt{2}$ and $(|\uparrow\downarrow\rangle - |\downarrow\uparrow\rangle)/\sqrt{2}$, will not generate contributions in the other two sectors up to second order in time-dependent perturbation theory. The detailed treatment of perturbation theory, which is long and tedious, can be matched term by term to the time evolution given by an effective Hamiltonian of the form:

$$\begin{aligned}
H_{eff} &= \sum_{i \neq I, I-1, I+1} \frac{J_i}{2} (S_i^+ S_{i+1}^- + S_i^- S_{i+1}^+ + 2\Delta_i S_i^z S_{i+1}^z) \\
&\quad + h\tilde{S}_D^z + \frac{J_{I-1}J_{I+1}}{2J_I(1-\Delta_I^2)} (S_{I-1}^+ S_{I+1}^- + S_{I-1}^- S_{I+1}^+) \\
&\quad + \frac{\Delta_I J_{I-1} J_{I+1}}{2J_I} \left[\frac{S_{I-1}^+ S_{I+1}^- + S_{I-1}^- S_{I+1}^+}{1-\Delta_I^2} - \frac{\Delta_{I-1}\Delta_{I+1}}{\Delta_I} S_{I-1}^z S_{I+1}^z \right] \tilde{S}_D^z \\
&= H_{rest} + H_{I-1, I+1}. \tag{5}
\end{aligned}$$

The first sum in Eq. (5), called H_{rest} , is equal to the original Hamiltonian, excluding the strongest bond and the two neighboring ones. The three remaining terms of Eq. (5), included in $H_{I-1, I+1}$, effectively couple the spins neighboring the strong bond. The degrees of freedom of the strong bond (at I) contribute through \tilde{S}_D^z , where the subindex D stands for ‘‘decimated bond’’. As seen earlier, second order time-dependent perturbation theory does not allow the states $|\uparrow\uparrow\rangle$ and $|\downarrow\downarrow\rangle$ in positions $I, I + 1$ to appear, and therefore that region of the Hilbert space can be neglected. The spins in positions $I, I + 1$ therefore effectively oscillate in the subspace of $|+\rangle \equiv (|\uparrow\downarrow\rangle + |\downarrow\uparrow\rangle)/\sqrt{2}$ and $|-\rangle \equiv (|\uparrow\downarrow\rangle - |\downarrow\uparrow\rangle)/\sqrt{2}$, where they are *locked* in anti-aligned configurations, starting with $|\uparrow\downarrow\rangle = (|+\rangle + |-\rangle)/\sqrt{2}$. The operator \tilde{S}_D^z is defined as the spin

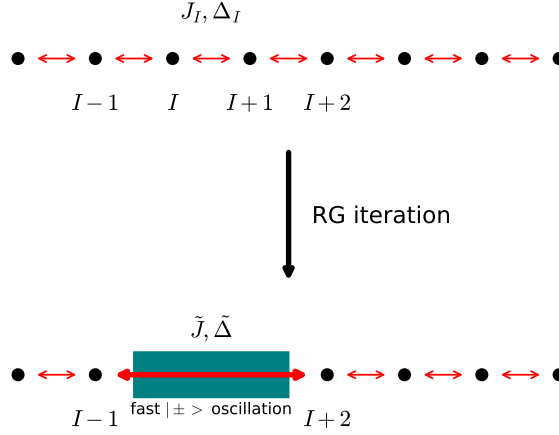


Figure 2: Representation of the decimation of the strongest bond in the chain, at site I . Sites $I - 1$ and $I + 2$ are effectively coupled through \tilde{J} and $\tilde{\Delta}$, which are computed after a second order time-dependent perturbation theory evolution of the original state.

operator of this degree of freedom: $\tilde{S}_D^z |+\rangle = 1/2 |+\rangle$ and $\tilde{S}_D^z |-\rangle = -1/2 |-\rangle$. Note that, as discussed above, the time evolution does not generate terms outside the subspaces $|+\rangle$ and $|-\rangle$ for positions I and $I + 1$.

The effective Hamiltonian in Eq. (5) commutes with the operator \tilde{S}_D^z , and so the time evolution of the wave function of the system in the $|+\rangle$ sector and that one in the $|-\rangle$ sector are completely independent (non-interacting), and they can be studied separately. By substituting \tilde{S}_D^z by either $\pm 1/2$ one gets a Hamiltonian of the form of Eq. (1) for the chain, plus a constant term $h\tilde{S}_D^z$. The sites $I, I + 1$ have been effectively removed, or decimated, and the spins on sites $I - 1, I + 2$ are now coupled through renormalized constants:

$$\begin{aligned} \tilde{J} &\equiv \frac{J_{I-1}J_{I+1}}{J_I(1 - \Delta_I^2)} \left(1 + \Delta_I \tilde{S}_D^z\right) \\ \tilde{\Delta} &\equiv -\Delta_{I-1}\Delta_{I+1} \frac{1 - \Delta_I^2}{4(1 + \Delta_I \tilde{S}_D^z)}. \end{aligned} \quad (6)$$

The decimation of the strongest bond in the chain, which represents the SDRG move, has to be applied iteratively. Since the interaction parameter is $|\Delta_i| < 1$, the different Δ 's obtained in the RG will flow to 0, and it is justified

to approximate the renormalized parameters in Eq. (6) by:

$$\begin{aligned}\tilde{J} &\equiv \frac{J_{I-1}J_{I+1}}{J_I} = \frac{J_{I-1}J_{I+1}}{\Omega} \\ \tilde{\Delta} &\equiv -\frac{\Delta_{I-1}\Delta_{I+1}}{4}.\end{aligned}\tag{7}$$

The process of decimating the strongest bond is represented in Fig. 2.

3.3 Flow of the probability distribution of the parameters of the strongest bond

The RG rules for the renormalized parameters described in Eq. (7) tell us that, at a particular RG step, the effective strength of the coupling and interaction parameters between the neighbor to the left of site I and to the right of site $I+1$ are given as a function of the three couplings and interaction terms between the four sites involved in the RG move. The parameters were at first generated randomly from uncorrelated distributions, and so the updated parameters are also random variables. A detailed study of the SDRG involves the probability of, at a particular step at time t , finding a particular value of Ω , J and Δ , although it is worth noting before proceeding that the variables t and Ω are clearly not independent, but rather $\Omega/\Omega_0 = \Omega t$, where Ω_0 is the value of Ω at time 0.

This problem was originally solved in Ref. [3] through the changes of variables: $\zeta = \log(\Omega/J)$, $\beta = -\log(|\Delta|)$ and $\Gamma = \log(\Omega_0 t)$. The resulting probability distribution, $P(\zeta, \beta; \Gamma)$ follows a time evolution given by the integral equation:

$$\begin{aligned}\frac{\partial P}{\partial \Gamma} &= \frac{\partial P}{\partial \zeta} + \rho(0; \Gamma) \int_0^\infty d\beta_{I-1} d\beta_{I+1} d\zeta_{I-1} d\zeta_{I+1} \delta(\zeta - \zeta_{I-1} - \zeta_{I+1}) \\ &\quad \delta(\beta - \beta_{I-1} - \beta_{I+1} - \log(4)) P(\zeta_{I-1}, \beta_{I-1}; \Gamma) P(\zeta_{I+1}, \beta_{I+1}; \Gamma).\end{aligned}\tag{8}$$

Studying Eq. (8) is beyond the scope of this paper, but it is worth noting that such a treatment provides interesting insight on the problem, and more precise results than the more qualitative Section 4. Furthermore, it is possible to extract information from the dynamical fixed point of this time evolution, *i.e.* the stationary solution to Eq. (8).

4 Results

In Ref. [7] the results are based on the analysis of Eq. (8). As mentioned in Section SDRG, this provides very interesting results on the strong disorder MBL

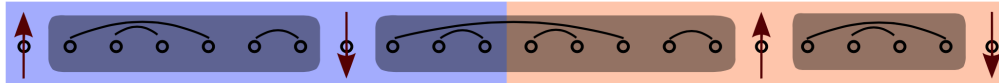


Figure 3: Depiction of the chain after some RG steps. At first the decimated sites are nearest neighbors, but at later times they are far apart, with already decimated pairs in between. The interface between the left and right subsystems cuts a number of the effective bonds, which is proportional to the entanglement entropy between subsystems.

phase. However, there is a simpler way of analyzing the SDRG procedure and still get powerful results. This involves an inspection of time evolution of the initial state $|\psi\rangle_0$ following the decimation procedure described in Section 3. First, note that a key point in the SDRG is the fact that at each step the strongest coupling $J_I = \Omega$ is considered to be much bigger than the second to strongest. This is not a strong assumption on the parameters of the system, but rather it is the case for the distribution of the coupling constants as the system flows to a fixed point of infinite randomness. If the system does not flow to infinite randomness, but to a distribution of strong disorder, the error made by the previous assumption is under control, and such an approximation is justified. For that reason, at each time step we can consider that time scales (Ω^{-1}) much larger than the ones considered in previous iterations are being accessed. If the ratio of Ω at a certain step in the SDRG procedure to its value in the previous step is constant for different steps, then the time scales follow a multiplicative recursion relation and the time scales grow exponentially, which implies that t in the time evolution increases exponentially with RG iterations. In other words:

$$t \propto \exp(n) \Rightarrow n \propto \log(\Omega_0 t), \quad (9)$$

where n is the RG step considered. If the ratio of the Ω 's is not kept constant, it can still be considered upper bounded due to the assumption on the coupling constants discussed earlier in this paragraph; in that case, Eq. (9) can be considered as a bound.

Second, the physical properties of the system are controlled by the decimation of pairs of sites at different times. As can be seen in Fig. 3, the decimation occurs first between nearest neighbors, but at later times it can occur between sites that are far apart from each other, if the sites between them have already been decimated.

Let's compute the evolution of the von Neumann entanglement entropy

between the left half of the system and the right half. The entanglement entropy provides an interpolation of the measurement of entanglement between situation in which pairs of qubits are maximally entangled. It can therefore be regarded as the amount of pairs of qubits that are entangled between two subsystems. As can be seen in Fig. 3, the interface between both subsystems cuts a number of the effective bonds between decimated sites. Each bond represents a pair spins that are locked and oscillating in the subspace of anti-aligned states between the maximally entangled $|+\rangle$ and $|-\rangle$, going through the not entangled states $|\uparrow\downarrow\rangle$ and $|\downarrow\uparrow\rangle$ (see Section 3.2). Therefore, each bond contributes to the (time averaged) entanglement entropy between both subsystems by a non-zero amount S_p , which is smaller than the maximum 1. S_p is independent of the bond and of the RG step in which that bond was generated. We now have to count the number of such bonds for a particular time t . It is easy to realize that at each RG step n , the decimated pair of sites is 1 among $N_n - 1$ remaining pairs, where N is the number of sites that have not been decimated yet. The number of bonds going through the interface between both subsystems at step n is proportional to the integral bounded by a function linear in n . To be more precise, the renormalized \tilde{J} on the bond that crosses the interface after a step in which the decimated bond also crossed the interface is particularly small, due to Eq. (7); therefore, the probability of choosing this bond in the current decimation is very low, and the actual growth of the number of bonds with step n is slower than the naive linear one. In turn, the entanglement entropy growth across the two halves of the system is bounded by a logarithmic growth in time, t , which is observed in numerical simulations. Note that this is different from the linear growth for generic systems. This is a striking result of the SDRG. In Ref. [7], the more detailed calculation carried gives a growth for the entanglement entropy that scales as $\log(\log(\Omega_0 t))$, tighter than the bound proposed here.

Following arguments, it is easy to analyze the decay of the staggered magnetization of the original antiferromagnetic state. Every pair of decimated spins contributes a time average of 0 to the staggered magnetization, which is maximal for completely anti-aligned spins. At each RG step, one pair of spins is removed from the contribution to the staggered magnetization. In the thermodynamic limit and at long times, the contributions to the staggered magnetization left on the system scale as $1/\log^2(\Omega_0 t)$. This result is also observed numerically, and is qualitatively different from the exponential decay in the clean XXZ model.

Finally, the average length of the bonds between the effective spins left in the system is proportional to the inverse of the staggered magnetization, or to the inverse of the effective spins left. For that reason, it scales grows as $\log^2(\Omega_0 t)$. This slow propagation of correlation is in agreement with compu-

tational studies, and contrasts with the usual propagation of information in a quantum system, which is linear in time (with an effective “light cone” given by the Lieb-Robinson bound).

5 Conclusions

In this paper we have seen a dynamical RG approach to the problem of many-body localization. Rather than analyzing the transition between an ergodic and an MBL phase, the dynamical properties of an MBL phase due to strong disorder are studied. The original study of Ref. [7] relies on the analysis of the integral Eq. (8), while in this paper we rely on less detailed arguments to reproduce qualitative results.

A logarithmic bound for the growth of the entanglement entropy between two subsystems is found, which is in agreement to the usual numerical results for similar systems. A $1/\log(t)$ decay of the staggered magnetization is also found, as well as a $\log(t)$ growth of the length of the effective bonds in the system, results that are also in agreement with computational simulations of similar systems.

It is interesting how the SDRG gives theoretical arguments to obtain result that are in great agreement with the numerical simulations. Numerical simulations of quantum systems are very much constrained by the size of the systems studied, and the results obtained are often subject to being carefully scrutinized, since they are far from offering a reliable extrapolation to the thermodynamic limit. The insight that RG techniques like the SDRG can give to problems that are otherwise intractable makes them extremely valuable.

References

- [1] Jae-yoon Choi, Sebastian Hild, Johannes Zeiher, Peter Schauß, Antonio Rubio-Abadal, Tarik Yefsah, Vedika Khemani, David A Huse, Immanuel Bloch, and Christian Gross. Exploring the many-body localization transition in two dimensions. *Science*, 352(6293):1547–1552, 2016.
- [2] Daniel S Fisher. Random transverse field ising spin chains. *Physical review letters*, 69(3):534, 1992.
- [3] Daniel S Fisher. Random antiferromagnetic quantum spin chains. *Physical review b*, 50(6):3799, 1994.
- [4] Daniel S Fisher. Critical behavior of random transverse-field ising spin chains. *Physical review b*, 51(10):6411, 1995.

- [5] David J Luitz and Yevgeny Bar Lev. The ergodic side of the many-body localization transition. *arXiv preprint arXiv:1610.08993*, 2016.
- [6] Michael Schreiber, Sean S Hodgman, Pranjal Bordia, Henrik P Lüschen, Mark H Fischer, Ronen Vosk, Ehud Altman, Ulrich Schneider, and Immanuel Bloch. Observation of many-body localization of interacting fermions in a quasirandom optical lattice. *Science*, 349(6250):842–845, 2015.
- [7] Ronen Vosk and Ehud Altman. Many-body localization in one dimension as a dynamical renormalization group fixed point. *Physical review letters*, 110(6):067204, 2013.
- [8] Ronen Vosk and Ehud Altman. Dynamical quantum phase transitions in random spin chains. *Physical review letters*, 112(21):217204, 2014.